AJNR

Hyperintensities of the Optic Radiation on T2-Weighted MR Images of Elderly Subjects

Mika Kitajima, Yukunori Korogi, Tomoko Okuda, Shin-ya Shiraishi, Osamu Ikeda, Shoji Morishita, Mutsumasa Takahashi and Komyo Eto

Hyperintensities of the Optic Radiation on T2-Weighted MR Images of Elderly Subjects

Mika Kitajima, Yukunori Korogi, Tomoko Okuda, Shin-ya Shiraishi, Osamu Ikeda, Shoji Morishita, Mutsumasa Takahashi, and Komyo Eto

BACKGROUND AND PURPOSE: Although abnormal hyperintensities are frequently observed at or around the optic radiation in elderly subjects, no previous reports have mentioned the clinical significance and pathologic changes of these hyperintensities. We evaluated the hyperintensity patterns of the optic radiation and its surrounding structures on T2-weighted MR images and compared these findings with pathologic observations and visual field measurements.

METHODS: High-resolution coronal T2-weighted MR images of 102 consecutive patients (51–84 years old) were evaluated retrospectively for the presence and morphology of hyperintensities of the optic radiation (204 sides) and its surrounding structures. Pathologic specimens were obtained from 25 other patients (60–91 years old) who had died of nonneurologic causes. The histopathologic changes of the optic radiation and its surrounding structures were evaluated and correlated with the MR findings. Finally, MR findings and visual field measurements were correlated in 46 elderly volunteers (70–91 years old).

RESULTS: Hyperintensities of the optic radiation or its surrounding structures or both were observed on 125 sides (93%) of 67 patients (61%), and linear/laminar hyperintensity of the optic radiation and the tapetum was the characteristic finding. Eleven (44%) of 25 pathologic specimens exhibited pallor of three anatomic layers (the external sagittal stratum or the optic radiation, the internal sagittal stratum, and the tapetum). No subjects with hyperintensity of the optic radiation had visual field abnormalities.

CONCLUSION: Linear/laminar hyperintensity of the optic radiation and tapetum on T2-weighted images is common in elderly subjects, and may reflect differences in the internal structures and in the water content of three anatomic structures. Hyperintensities of this region did not cause visual field abnormalities in a group of elderly volunteers.

The advent of MR imaging has brought attention to the high rate of occurrence of previously undetected morphologic brain abnormalities that cannot be related to gross clinical findings (1–6). These abnormalities appear hyperintense on both proton density– and T2-weighted images, and are commonly seen at the periventricular white matter and centrum ovale. Several groups have studied the histopathologic correlation between these hyperintensities with in vivo and postmortem MR findings,

and various histologic changes have emerged. Proposed correlates include extensive areas of demyelination and axonal loss, atrophy of perivascular myelin, infarcts, and dilated perivascular spaces (7–13).

Abnormal hyperintensities are also frequently observed at or around the optic radiation in elderly subjects, just like the periventricular hyperintensities of other regions. However, we noted that these hyperintensities tended to be linear or laminar in shape; therefore, we undertook this study to discover the histopathologic changes of these hyperintensities and to learn why these hyperintensities are laminar in shape. We also questioned whether these laminar hyperintensities cause visual field deficits. No previous reports have mentioned the relationship between these hyperintensities and the optic radiation or visual field abnormalities. To address this issue, we compared MR images of elderly subjects with pathologic specimens of corresponding regions of the brain. We also evaluated

the relationship of these hyperintensities to their visual fields.

Methods

This study was conducted in three parts: evaluation of high-resolution fast spin-echo T2-weighted MR images; analysis of neurohistopathologic specimens; and correlation of MR findings with visual field measurements.

Evaluation of High-Resolution Fast Spin-Echo T2-Weighted MR Images

The MR images of 102 consecutive patients were evaluated retrospectively. Fifty-eight patients were men and 44 were women. Ages ranged from 51 to 84 years (mean, 68 years): 23 (13 men and 10 women) were 51 to 59 years old; 50 (29 men and 21 women) were 60 to 69 years old; 21 (11 men and 10 women) were 70 to 79 years old; and eight (five men and three women) were 80 to 84 years old. The indications for MR imaging included headache (n = 33), dizziness or stagger (n = 29), paresthesia (n = 12), gait disturbance (n = 8), syncope (n = 6), paresis (n = 4), dysarthria (n = 3), psychiatric problems (n = 2), transient amnesia (n = 2), tremor (n = 2), and tinnitus (n = 1). We excluded the patients with any abnormalities in the visual pathways (the optic nerve, optic chiasm, optic tract, lateral geniculate body, optic radiation, and striate cortex), malignancy, neurodegenerative disease, brain surgery, and acute stroke.

All patients were examined with a 1.5-T superconductive MR unit. Both axial and coronal T2-weighted fast spin-echo images were obtained with a high-resolution technique. Imaging parameters were 4000/112/2 (TR/TE/excitations) for axial images and 4000/128/2 for coronal images. The echo train length was 8 in both axial and coronal planes. The section thickness was 6.0 mm with a 2.5-mm intersection gap for axial images, 5 mm with a 1.5-mm intersection gap for coronal images. For axial images, the field of view was 23 × 17 cm, and the matrix was 512 × 256; for coronal images, the field of view was 23 × 23 cm, and the matrix was 512 × 256.

The MR findings of both hemispheres (204 sides) at the level between the trigone and posterior horn of the lateral ventricle were evaluated by two radiologists. Agreement was reached by consensus. By referring to the previous studies, the optic radiation was defined as a relatively hyperintense line on T2-weighted images parallel to the lateral ventricle with a maintained distance of 3 to 4 mm from the lateral ventricle (14, 15). Other structures around the optic radiation were defined as follows; the internal sagittal stratum was defined as the relatively hypointense line medial to the optic radiation, and the tapetum as the intermediately intense line medial to the internal sagittal stratum (14). The presence, severity, and morphology of the hyperintensity of the optic radiation and/or its surrounding structures, such as the internal sagittal stratum, the tapetum, and white matter, were evaluated on coronal T2-weighted images. The severity of these hyperintense foci was classified as mild, moderate, or severe. Mild was defined as focal patchy or thin linear hyperintensities, moderate as larger patchy or linear/laminar hyperintensities, and severe as thick laminar or diffuse involvement of periventricular white matter. The presence and the degree of nonspecific white matter lesions involving structures other than the optic radiation were also recorded on axial long TR/TE images. The degree of nonspecific white matter lesions was graded on a scale of 0 to 5 as follows (2): 0 = no lesions; 1 = punctate, minimal (<3) lesions; 2 = punctate, moderate (3–7) lesions; 3 = punctate, severe (>7) lesions; 4 = patchy focal lesions; 5 = coalescent lesions.

The presence of hypertension and diabetes was also recorded for the patients with hyperintensity of the optic radiation and/or its surrounding structures.

Analysis of Neurohistopathologic Specimens

Pathologic specimens from 25 consecutive patients (nine men and 16 women, mean age, 80 years; range, 60–91 years) who died of nonneurologic causes and were not previously studied with MR imaging were analyzed. Coronal sections were prepared at the level of the optic radiation, defined as the external sagittal stratum (15). Specimens were stained by the Klüver-Barrera method for the myelin sheaths and by the Bodian method for the axons. The degree of staining of the tapetum, internal sagittal stratum, external sagittal stratum, defined as the optic radiation, and adjacent white matter were assessed with the unaided eye or with low-power views on both stained specimens. With high-power magnification views, histopathologic changes of the three layers described above and adjacent white matter were evaluated. The histopathologic findings were evaluated by a neuropathologist. The presence of hypertension and diabetes was recorded from clinical data, and the presence of arteriosclerosis found at the brain cutting was recorded.

MR findings, including the location and extent of hyperintensities of the aforementioned 102 patients, were then compared with these 25 autopsy specimens.

Correlation of MR Findings with Visual Field Measurements

Forty-six elderly volunteers (21 men and 25 women, mean age, 77 years; range, 70–91 years) underwent both MR imaging and visual field measurement with Goldmann dynamic perimetry. Thirty-one patients (12 men and 19 women) were 70 to 79 years old, 14 (nine men and five women) were 80 to 89 years old, and one woman was 91 years old.

In this group, all patients were examined with a 1.5-T superconductive MR unit, and conventional coronal T2-weighted images were obtained. Imaging parameters for the conventional spin-echo T2-weighted images were 2200/80/1. Section thickness was 5.0 mm with a 1.1-mm intersection gap. The field of view was 25 × 25 cm, and the matrix was 256 × 192. Evaluation of MR images was done by two radiologists in the same manner as described for the high-resolution T2-weighted images.

Results

Evaluation of High-Resolution Fast Spin-Echo T2-Weighted MR Images

Hyperintensities of the optic radiation and/or its surrounding structures were observed in 67 (66%) of 102 patients. Fifty-eight patients had hyperintensity on both sides, and the remaining nine patients had lesions on one side only. Therefore, lesions existed in 125 (61%) of 204 sides. Of the 125 sides with hyperintensities, 49 sides showed hyperintensities in both the optic radiation and the tapetum, 48 sides in the optic radiation alone, and 24 sides in the tapetum alone. The remaining four sides showed patchy hyperintensities only in the white matter adjacent to the optic radiation. The age distribution of patients with hyperintensity of the optic radiation and/or its surrounding structures was as follows: eight patients (six men and two women) were 51 to 59 years old (8/21; 38%); 36 patients (24 men and 12 women) were 60 to 69 years old (36/50; 72%); 15 patients (nine men and six women) were 70 to 79 years old (15/21; 71%); and eight patients (five men and three women) were 80 to 84 years old (8/8; 100%) (Fig 1).

The hyperintensities were mild on 73 sides (58%) (Fig 2A), moderate on 35 sides (28%), and
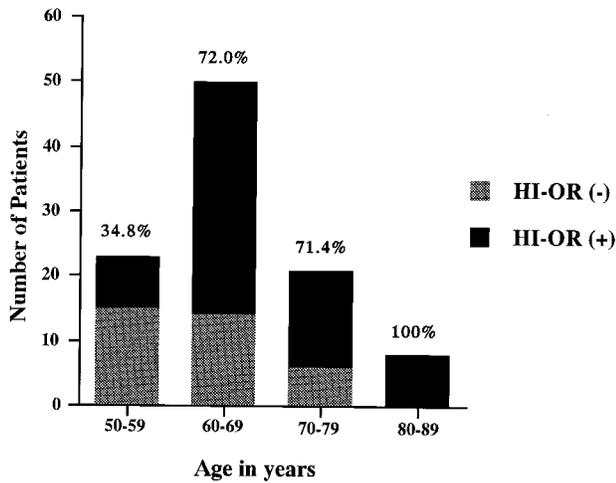
FIG 1. Age-specific prevalence (%) of hyperintensities of the optic radiation and/or its surrounding structures increases with age. *HI-OR* indicates hyperintensity at or around the optic radiation.
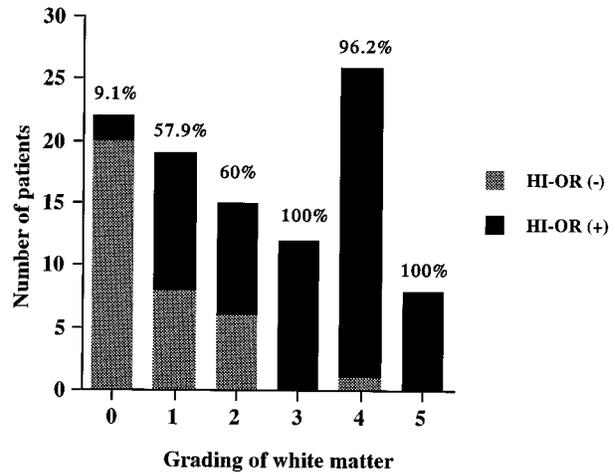

FIG 3. Relationship between the grade of white matter hyperintensities and the number of patients in each group. The frequency (%) of hyperintensity of the optic radiation and/or its surrounding structures correlated well with severity of other white matter hyperintensities. *HI-OR* indicates hyperintensity at or around the optic radiation.

severe on 17 sides (14%) (Fig 2B). The linear/laminar hyperintensity of the optic radiation and tapetum, the most characteristic feature in this area, was observed on 94 (75%) of 125 sides.

Nonspecific white matter lesions in sites other than the optic radiation were observed in 65 (97%) of the patients with hyperintense foci of the optic radiation. The distribution of grades for these nonspecific white matter lesions was as follows: grade 0 was observed in two patients, grade 1 in 11 patients, grade 2 in nine patients, grade 3 in 12 patients, grade 4 in 25 patients, and grade 5 in eight patients. The frequency and severity of hyperintensity of the optic radiation and/or its surrounding structures correlated well with the severity of the white matter hyperintensities (Fig 3).

Hypertension was present in 29 patients (43%), and diabetes was found in nine patients (13%).

Analysis of Neurohistopathologic Specimens

Eleven (44%) of 25 specimens exhibited abnormalities of the optic radiation and/or its surrounding structures. With the unaided eye or low-power microscopic evaluation of the abnormal specimens, the three layers (the external sagittal stratum or the optic radiation, internal sagittal stratum, and tapetum) were pale relative to normal specimens. The external sagittal stratum was more strongly stained than were the internal sagittal stratum and tapetum (Fig 4A and B). In three of 11 specimens, the distinctiveness of the three layers was lost (Fig 4B). One specimen showed thinning of three layers with ventricular dilatation (Fig 4C). The histopathologic changes in the white matter lateral to the external sagittal stratum included patchy pallor lesions and infarction (see Fig 4B). The former was observed in eight specimens and the latter in two specimens.

On high-power microscopic evaluation of these three layers, a decrease of myelinated fibers in the areas of the pallor lesions was observed. Dilated perivascular spaces were seen in two specimens, localized ischemic change surrounding an arteriole with arteriosclerosis in one specimen, and infarction involving both the external and sagittal stratum in one specimen.
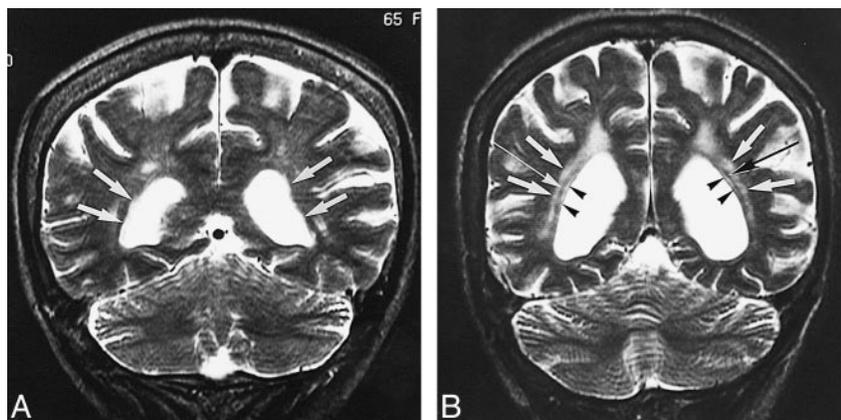

FIG 2. *A,* Coronal high-resolution T2-weighted image (4000/128/2) of a 65-year-old woman shows linear hyperintensities of the tapetum on both sides (*arrows*).

B, Coronal high-resolution T2-weighted image (4000/128/2) of a 78-year-old woman shows thick laminar hyperintensity of the optic radiation (*short arrows*) and other linear hyperintensities of the tapetum (*arrowheads*) on both sides. The hypointense structure between the optic radiation and the tapetum is the internal sagittal stratum (*long arrows*).
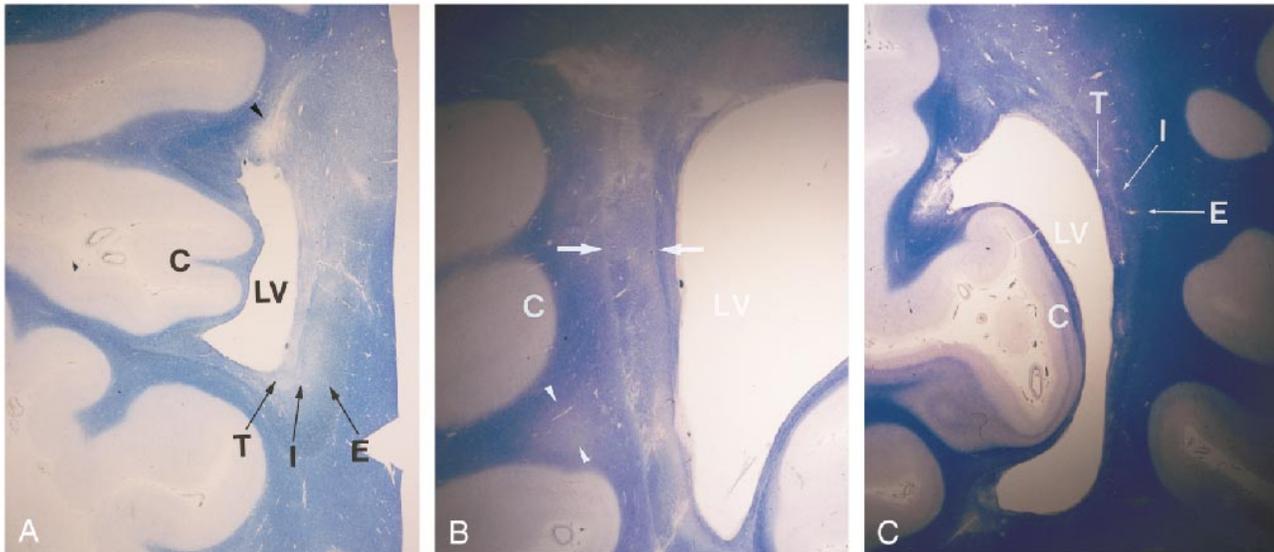
FIG 4.   *A,* Coronal specimen from an 88-year-old woman shows blurring of the three layers: external sagittal stratum or the optic radiation (*E*), internal sagittal stratum (*I*), and tapetum (*T*). All three layers are pale relative to adjacent white matter. Infarcted area is also observed at the superior periventricular white matter (*arrowhead*). *LV* indicates lateral ventricle; *C,* medial occipital cortex. Klüver-Barrera method, original magnification × 4.

B, Coronal specimen from a 73-year-old man shows loss of distinction between the external sagittal stratum or the optic radiation and the internal sagittal stratum (*arrows*). This area is pale relative to adjacent white matter. Patchy pallor lesions are also observed in the white matter adjacent to the external sagittal stratum (*arrowheads*). *LV* indicates lateral ventricle; *C,* lateral occipital cortex. Klüver-Barrera method, original magnification × 4.

C, Coronal specimen from a 79-year-old man shows thinning of the three layers: external sagittal stratum or the optic radiation (*E*), internal sagittal stratum (*I*), and tapetum (*T*). *LV* indicates lateral ventricle; *C,* medial occipital cortex. Klüver-Barrera method, original magnification × 4.

Associated hypertension was found in eight of 25 patients, diabetes in two patients, and arteriosclerosis in eight patients.

Correlation of MR Findings with Visual Field Measurements

Hyperintensities of the optic radiation and/or its surrounding structures were observed on 66 sides (72%) of 34 subjects (74%). Thirty-two subjects had hyperintensity on both sides, and the remaining two had hyperintensity on one side. Of 66 sides with hyperintensities, 24 sides showed hyperintensities in both the optic radiation and the tapetum, 23 sides in the optic radiation alone, and 14 sides in the tapetum alone. The remaining five sides showed patchy hyperintensities only in the white matter adjacent to the optic radiation. The age distribution of subjects with hyperintensity of the optic radiation and/or its surrounding structures was as follows: 20 patients (nine men and 11 women) were 70 to 79 years old (20/31; 65%); 13 (eight men and five women) were 80 to 89 years old (13/14; 93%); and one woman was 91 years old (1/1; 100%). The hyperintensities of the optic radiation were mild on 24 sides (36%), moderate on 24 sides (36%), and severe on 18 sides (27%). None of the subjects showed visual field abnormalities on Goldmann dynamic perimetry.

Nonspecific white matter lesions other than in the optic radiation were observed in all 34 patients with hyperintensity of the optic radiation and/or its surrounding structures. The grade of these nonspecific white matter lesions was as follows: grade 0 was not observed in any patient, grade 1 was seen in three patients, grade 2 in one patient, grade 3 in 10 patients, grade 4 in 16 patients, and grade 5 in four patients. The grades of white matter hyperintensity and of hyperintensity of the optic radiation and/or its surrounding structures were well related.

Discussion

In the occipital periventricular region, three anatomic structures exist parallel to the lateral ventricular wall. From lateral to medial, they include the external sagittal stratum, also known as the optic radiation, the internal sagittal stratum, which contains fibers from the colliculus, and the tapetum, which consists of fibers from the corpus callosum. Histologically, the external sagittal stratum is large and separated by wide translucent spaces, whereas the internal sagittal stratum is more compact. These histologic findings result, in part, in their characteristic signal intensity. The external sagittal stratum or the optic radiation appears relatively hyperintense on T2-weighted images and relatively hypointense on T1-weighted images, whereas the internal sagittal stratum is relatively hypointense on T2-weighted images (14). Involvement of the optic radiation by pathologic conditions, such as an infarction or a neoplastic lesion, causes visual field deficits that correspond to the involved region of the optic radiation. Involvement of the upper part

of the optic radiation results in lower quadrantic hemianopsia, and involvement of the lower part of the optic radiation results in upper quadrantic hemianopsia.

There have been many studies of nonspecific periventricular or deep white matter hyperintensities seen on T2-weighted MR images in elderly subjects (1–6). Such hyperintensities in elderly subjects have been observed to vary from 30% to 94%, with most authors reporting more than 75% (2–6). They are classified according to their location and shape; for example, triangular caps around the frontal horns; thin, smooth periventricular rims; and patchy, periventricular hyperintensities. Histologic findings of these hyperintensities include myelin pallor, gliosis, loss of the ependymal lining, dilated perivascular spaces, and perivascular gliosis (7–13).

In the present study, the frequency of hyperintensities in the optic radiation and/or its surrounding structures was 66% in patients older than 50 years of age, increased with age (Fig 1), and were associated with the presence and severity of other white matter hyperintensities (Fig 3). White matter lesions and abnormalities of the optic radiation were observed more frequently in the group studied with conventional spin-echo imaging than in those studied with fast spin-echo imaging. Some factors may be related to this difference. First, it is known that fast spin-echo images with a long TR serve to decrease the conspicuity of white matter abnormalities. Similarly, fast spin-echo images may be less sensitive for detecting abnormalities of the optic radiation. Second, the mean age was older in the group studied with conventional spin-echo imaging than in the those examined with fast spin-echo imaging. Third, the pixel size was different in these two groups: it was 0.45×0.9 mm for the fast spin-echo sequences and 0.98×1.3 mm for the conventional spin-echo sequences. We think that the most significant factor contributing to the difference in the frequency of hyperintensities between the two groups was the age of the subjects.

In this study, linear/laminar hyperintensities of the optic radiation and tapetum were the most characteristic features on MR images. However, our histologic specimens did not show preferential involvement of the optic radiation; rather, all three layers were involved. In the studies of correlation between pre- and postmortem MR images by Fazekas et al (13), the white matter hyperintensities were better delineated on premortem MR images than on postmortem ones. MR images before death seem to have a higher sensitivity for these hyperintensities than do findings observed with the unaided eye on postmortem histologic specimens. We believe that a similar mechanism may account for the discrepancy we found between MR findings and unaided-eye findings on pathologic specimens in delineating abnormalities of the optic radiation.

There are several hypotheses of the formation of periventricular hyperintensities. Among them, increase of water content and altered periventricular fluid dynamics are the important mechanisms (16–19). In the study of magnetization transfer imaging by Wong et al (16), the periventricular hyperintensities had a lower magnetization transfer ratio, reflecting the increased water content in reactive gliosis. An increase in periventricular water was caused by various factors, including breakdown of ependymal lining, natural flow of intercellular water toward the lateral ventricles (17, 18), and higher venous filtration pressure caused by slow progression of stenosis or occlusion of deep cerebral veins (19). It has been shown that histologic change caused by these conditions is similar to white matter edema (20, 21). White matter edema appears in the white matter, but does not involve the subcortical U fibers (20). Because the subcortical U fibers have more compact myelin than other white matter, the subcortical U fibers are relatively resistant to white matter edema. Histologic differences between the external sagittal stratum and the internal sagittal stratum are similar to those between the white matter and the subcortical U fibers. The optic radiation associated with loosely compacted myelin tends to be affected by a relative increase of fluid, whereas the internal sagittal stratum, with compact translucent spaces, may be resistant to an increase of fluid. Our results may support this hypothesis, as linear/laminar hyperintensities were not observed at the region of the internal sagittal stratum but at the external sagittal stratum or the optic radiation and tapetum.

The histologic changes of the patchy hyperintensities adjacent to the optic radiation, consisting of myelin pallor, dilated perivascular spaces, perivascular gliosis, and small ischemic changes surrounding arteriosclerosis of small arteriole, were similar to those in other periventricular white matter regions. The diffuse hyperintensity probably corresponds to diffuse pallor involving all three layers and the adjacent white matter. Hyperintensities of the optic radiation and/or its surrounding structures were accompanied by other white matter hyperintensities in almost all patients. Therefore, it would appear to be the same pathologic condition, and probably is caused by an increase of water content and altered fluid dynamics.

The clinical significance of periventricular or deep white matter hyperintensities is controversial. In most studies to date, neurologic test findings have shown no correlation with hyperintensity foci (22–26). Nevertheless, a study by Baum et al (27) reported that white matter foci were found to be related to performance on immediate visual memory/visuoperceptual skills and on visuomotor tracking/psychomotor speed. In our study, hyperintensities involving the optic radiation did not cause visual field abnormalities on Goldmann dynamic perimetry, although other visual functions, such as color vision or visual associated function, were not evaluated. It is possible that visual functions other than visual field might have been disturbed in sub-

jects with hyperintensities of the optic radiation and/or its surrounding structures.

The differential diagnosis of hyperintensities of the optic radiation include infarction and wallerian degeneration of the optic radiation. Wallerian degeneration is always accompanied by other lesions of the visual pathway. The presence and morphologic characteristics of accompanying lesions of the visual pathway were the keys to differentiating these conditions from the hyperintensities identified in the present study.

Our study was limited by the lack of direct correlation between MR and histopathologic findings in the same patients. Nevertheless, the histopathologic specimens correlated nicely with the common findings in our elderly subjects. We believe that close correlation between MR and histologic findings in the same-age group of patients is a useful method to understand MR observations better.

Conclusion

Linear/laminar hyperintensities of the optic radiation and tapetum are common in elderly subjects. These hyperintensities may be caused by several pathologic changes, including myelin pallor, small infarction or ischemic lesions or both, and dilated perivascular spaces. An increase of water content and altered fluid dynamics have been implicated as important mechanisms for these hyperintensities. The laminar anatomic structures (the external sagittal stratum, internal sagittal stratum, and tapetum) seem to correspond to these laminar hyperintensities, and the external sagittal stratum, with its loosely compacted myelin, is the most preferentially affected region. These hyperintensities do not cause visual field abnormalities.

References

1. Heierl LA, Bauerl CJ, Schwartz L, Zimmermanl RD, Morgello S, Deck MDF. **Large Virchow-Robin spaces: MR-clinical correlation.** *AJNR Am J Neuroradiol* 1989;10:929–936
2. Awad IA, Spetzler RF, Hodak JA, et al. **Incidental lesions identified on magnetic resonance imaging in the elderly, I: correlation with age and cerebrovascular risk factors.** *Stroke* 1986;17:1084–1089
3. Gerard G, Weisberg L. **MRI periventricular lesions in adults.** *Neurology* 1986;36:998–1001
4. Sarpel G, Chaudry F, Hindo W. **Magnetic resonance imaging of periventricular hyperintensity in a Veterans Administration hospital population.** *Arch Neurol* 1987;44:725–728
5. Zimmerman RD, Fleming CA, Lee B, et al. **Periventricular hyperintensity as seen by magnetic resonance: prevalence and significance.** *AJNR Am J Neuroradiol* 1986;7:13–20
6. George AE, de Lenou MJ, Kalnin A, et al. **Leukoencephalopathy in normal and pathologic aging, 2: MRI of brain lucencies.** *AJNR Am J Neuroradiol* 1986;7:567–570
7. Fazekas F, Kleinert R, Offenbacher H, et al. **Pathologic correlates of incidental MRI white matter signal hyperintensities.** *Neurology* 1993;43:1683–1689
8. Leifer D, Buonanno FS, Richardson EP. **Clinicopathologic correlations of cranial magnetic resonance imaging of periventricular white matter.** *Neurology* 1990;40:911–918
9. Chimowitz MI, Estes ML, Furlan AJ, Awad IA. **Further observations on the pathology of subcortical lesions identified on magnetic resonance imaging.** *Arch Neurol* 1992;49:747–752
10. Munoz DG, Hastak SM, Harper B, Lee D, Hachinski VC. **Pathologic correlates of increased signals of the centrum ovale on magnetic resonance imaging.** *Arch Neurol* 1993;50:492–497
11. Braffman BH, Zimmerman RA, Trojanowski JQ, Gonatas NK, Hickey WF, Schlaepfer WW. **Brain MR: pathologic correlation with gross and histopathology, 1: lacunar infarction and Virchow-Robin spaces.** *AJNR Am J Neuroradiol* 1988;9:621–628
12. Braffman BH, Zimmerman RA, Trojanowski JQ, Gonatas NK, Hickey WF, Schlaepfer WW. **Brain MR: pathologic correlation with gross and histopathology, 2: hyperintense white-matter foci in the elderly.** *AJNR Am J Neuroradiol* 1988;9:629–636
13. Fazekas F, Kleinert R, Offenbacher H, et al. **The morphologic correlate of incidental punctate white matter hyperintensities on MR images.** *AJNR Am J Neuroradiol* 1991;12:915–914
14. Kitajima M, Korogi Y, Takahashi M, Eto K. **MR signal intensity of the optic radiation.** *AJNR Am J Neuroradiol* 1996;17:1379–1383
15. Talmage LP. **The visual pathway and the occipital lobe.** In: Talmage LP, ed. *The Neuroanatomic Basis for Clinical Neurology.* 3rd ed. New York: McGraw-Hill; 1977:469–502
16. Wong KT, Grossman RI, Boorstein JM, et al. **Magnetization transfer imaging of periventricular hyperintense white matter in the elderly.** *AJNR Am J Neuroradiol* 1995;16:253–258
17. Hochwald GM, Wald A, Malhan C. **The risk action of cerebrospinal volume flow.** *Arch Neurol* 1976;33:339–344
18. Pollay M, Curl F. **Secretion of cerebrospinal fluid by ventricular ependyma of the rabbit.** *Am J Physiol* 1967;213:1031–1038
19. Moody DM, Brown WR, Challa VR, Anderson RL. **Periventricular venous collagenosis: association with leukoaraiosis.** *Radiology* 1997;194:469–476
20. Lorenzo AV, Bresnan MJ, Barlow CF. **Cerebrospinal fluid absorption deficit in normal pressure hydrocephalus.** *Arch Neurol* 1974;30:387–392
21. Takami N, Shirakuni T, Ehara K, Matsumoto S. **Characterization of periventricular edema in normal-pressure hydrocephalus by measurement of water proton relaxation times.** *J Neurosurg* 1990;73:864–870
22. Almkvist O, Wahlund LO, Anderson Lundman G, Bausn H, Bèckman L. **White-matter hyperintensity and neuropsychological function in dementia and healthy aging.** *Arch Neurol* 1992;49:626–632
23. Hunt AL, Orrison WW, Yeo RA, et al. **Clinical significance of MRI white matter lesions in the elderly.** *Neurology* 1989;39:1470–1474
24. Rao SM, Mittenberg W, Bernardin L, Haughton V, Leo GJ. **Neuropsychological test findings in subjects with leukoaraiosis.** *Arch Neurol* 1989;46:40–44
25. Schmidt R, Fazekas F, Offenbacher H, et al. **Magnetic resonance imaging white matter lesions and cognitive impairment in hypertensive individuals.** *Arch Neurol* 1991;48:417–420
26. Tupler LA, Coffey CE, Logue PE, Djang WY, Fagan SM. **Neuropsychological importance of subcortical white matter hyperintensity.** *Arch Neurol* 1992;49:1248–1252
27. Baum KA, Schulte C, Grike W, et al. **Incidental white-matter foci on MRI in healthy subjects: evidence of subtle cognitive dysfunction.** *Neuroradiology* 1998;38:755–760